

Hysteresis Behaviour and Specific Damping Capacity of Negative Poisson's Ratio Foams

Martz, E. O., Lakes, R. S., and Park, J. B. "Hysteresis behaviour and specific damping capacity of negative Poisson's ratio foams", *Cellular Polymers*, 15, 349-364, (1996).

Abstract

Open cell polyurethane foams have been previously made to be re-entrant, in that their cell ribs are inwardly bent, which results in the foam exhibiting a negative Poisson's ratio⁽¹⁾. Untransformed control and transformed negative Poisson's ratio foams were cyclically loaded at various levels of pre-strain to determine their hysteresis behavior, and from this, to elucidate its specific damping characteristics. Both untransformed and transformed foams exhibited non-linear hysteresis behavior at high cyclic strains, regardless of their initial levels of pre-strain. The specific damping capacity of the transformed foam with extreme compressive pre-strain was higher than that of the untransformed foam. This effect was attributed to the rubbing of the inwardly buckled cell ribs of the transformed foam. The specific damping capacity varied with both the level of pre-strain and with the amplitude of cyclic strain about that level.

Introduction

Poisson's ratio for a homogeneous, isotropic material under longitudinal load is defined as the negative of the ratio of lateral strain to longitudinal strain. Ordinary materials, including cellular solids, exhibit a positive Poisson's ratio, however, materials with a negative Poisson's ratio have been shown to exist⁽¹⁻⁵⁾. A method of transforming open cell foam such that it will then possess a negative Poisson's ratio has been demonstrated by one of the authors⁽¹⁾. The causal mechanism for this resultant negative Poisson's ratio is the inward buckling of the cell ribs of the foam, this has been described as having a "re-entrant" shape⁽¹⁾. Materials with a negative Poisson's ratio will show increased resilience and improved fracture toughness. Applications for such materials have been envisioned based on their unusual properties.

Viscoelastic materials are those in which the relationship between stress and strain depends on time or frequency. In dynamic (sinusoidal) loading of a linearly viscoelastic material, the relationship between stress and strain can be related by the loss tangent ($\tan \delta$). The loss angle represents the phase angle between the stress and strain sinusoids. The loss tangent, which depends upon frequency, is a measure of the viscoelastic damping of a material. When a linear viscoelastic material is cyclically loaded, the resulting stress vs. strain curve is an elliptic Lissajous figure, as shown in Figure 1(a). From this curve one can determine the loss angle [$\delta = \sin^{-1}(A/B)$]. For a nonlinear viscoelastic material, cyclic loading will result in a hysteresis loop which is not elliptic, for example the ones shown in Figure 1(b) or (c). For all viscoelastic materials the path of loading differs from the path of unloading. Polymeric materials can exhibit pronounced viscoelastic effects at ambient temperature.

Damping can be defined in several ways. $\tan \delta$ is an appropriate expression for linearly viscoelastic materials. For non-linear materials, a stress which is sinusoidal in time gives rise to a stress which is not sinusoidal, consequently a more general measure of damping is required. For example the specific damping capacity, referred to as η , is defined as the ratio of dissipated energy W_d to stored energy W_s per unit volume in cyclic loading. Such a ratio of energies has physical meaning regardless of the shape of the hysteresis loop.

$$\frac{W_d}{W_s} = \eta \quad (1)$$

in the general case can be related to $\tan \delta$ in the linear case by computation of the area within the elliptic curve in Figure 1(a). That area corresponds to dissipated energy W_d for a full cycle. The stored energy over a quarter cycle is computed as the area "opq" in Fig. 1 (a). Since the

material returns to its original values of stress and strain after each cycle it is not meaningful to speak of stored energy over a full cycle. $\tan \delta$ is related to η' via

$$\eta' = 2 \tan \delta \quad (2)$$

Since there are several possible ways of defining the stored energy, there are also several expressions for W (6). In the above, the stored elastic component of energy was used, in harmony with Ferry(7) and Nashif et al.(8). The slope of the line "op" forming the triangle used for calculation of area in Figure 1 (a) is the storage modulus E' , which is the real (in phase) part of the complex dynamic modulus. The quantity J' shown is the storage or in-phase compliance. It is also possible to consider as stored energy the total strain energy at maximum deformation or the total kinetic plus potential energies in vibrating systems with inertia(9).

Nonlinear viscoelastic materials will dissipate energy, but δ as a phase angle between sinusoids does not have the physical significance it does in linear materials, since nonlinearity causes the response to be non-sinusoidal. However, the energy ratio η'/E' will continue to have a meaningful physical interpretation despite the more complex shape of the hysteresis curve. The dissipated energy is proportional to the area within the curve regardless of its shape. Stored energy may be evaluated from the area of a triangle as was done for linear materials, but the slope of the hypotenuse corresponds to a secant modulus; see Figure 1 (c). Moreover, if the hysteresis loop is asymmetric, the slope is different for tension compared with compression. The area under an actual stress-strain curve should provide a more realistic value of the stored energy, but since the curves for loading and unloading are different there arises the question of what curve to use. One possibility is to construct a curve based the average of stress for loading and unloading, as represented by the dashed curve in Figure 1 (c).

Materials and Methods

Materials

Open cell polyurethane foams (Scott Industrial Foam, from Foamade Industries, Auburn Hills, MI) were used for these experiments as in earlier ones(1). The relative density, defined as the ratio (ρ/ρ_s) of the density ρ of the foam to the density ρ_s of the solid material composing the foam, was $0.03 \pm 7\%$. The length of the cell ribs of this foam was 1.2 mm. Sections were cut from the foam sample with dimensions as follows: 114.3 mm x 38.1 mm x 38.1 mm, and these sections were transformed into negative Poisson's ratio foam.

Processing

An aluminum tube of square cross section and inner dimensions 22 mm x 22 mm x 125 mm, was used as the mold, into which the foam specimens were inserted. The insertion resulted in compression in two transverse directions. Compression in the third direction was accomplished by applying an endplate (22 mm x 22 mm x 2.1 mm) to each end of the open ended aluminum tube. A series of spacers with a total length of 58.4 mm was used to compress the foam longitudinally; the combination of spacers and end plates was held in place using a clamping device. The mold assembly was placed in a furnace, which was heated to a predetermined temperature of 167°C. After the assembly had been heated for 19 minutes, it was removed from the furnace and allowed to cool to room temperature for an hour. The foam specimen was then removed and was gently stretched in the three orthogonal directions to eliminate any adhesion of the cell ribs.

Testing and analysis

A section (23 mm x 22 mm x 22 mm) was cut from the center of the transformed foam specimen, as well as from an untransformed foam sample, for hysteresis testing. The rationale for such a short column geometry was to prevent buckling in trials at high compressive strain. No

attempt was made to infer Young's modulus. The transformed foam was prepared with a permanent volumetric compression factor of 3.7, which based on previous work with this foam results in a Poisson's ratio of about -0.7⁽¹⁰⁾. The specimen was oriented with the 23 mm length as the longitudinal direction, parallel with the stroke of the testing machine. The center region was chosen because it exhibited the most visible effect in Poisson's ratio. The test coupons were fixed to smooth metal plates using a cyanoacrylate cement.

Stress vs. strain curves ranging from compression through tension were generated for both the untransformed and transformed samples by using a servohydraulic materials testing machine (Model 810, MTS Systems Corp., Minneapolis, MN). All tests were done in stroke control, with a sinusoidal waveform at a frequency of 1 Hz and at room temperature (20°C). Based on these curves, various strain levels were chosen about which cyclical loading was performed. Since the absolute values for strain were different in both the untransformed and transformed specimens, levels were chosen based on similar positions, relative to the stress vs. strain curve. About each level of strain, the sample was cyclically loaded at 4 successive strains (± 2 , ± 5 , ± 10 , and $\pm 15\%$ strain). Ten cycles were performed for each cyclic strain level. Values of initial strain ranged from extreme compression to extreme tension.

Results from the mechanical testing were recorded and plotted, and from these plots the ratio between energy dissipated and energy stored was determined. The area of the closed curve (representing the energy dissipated over a full cycle), and the area of the largest triangle (representing the energy stored over a quarter cycle associated with a secant modulus at peak stress), drawn from the origin of the cyclic strain, to the largest peak stress), were used to determine

. For comparison, some calculations were performed using a tangent approach represented by the area under the dashed curve in Figure 1 (c). These areas were plotted and then their shapes were cut out from the paper and weighed using an analytical balance. The ratio of their weights were then used to determine , since with constant thickness the ratio of their weights is identical to the ratio of their areas.

Results

Due to the large amount of data generated, it was decided to emphasize the extremes of the results obtained, namely, the cyclic loading of ± 2 and $\pm 15\%$ strain. The hysteresis loops for ± 2 and $\pm 15\%$ cyclic strain, for both the untransformed and transformed foams, are shown in Figures 2-5. All hysteresis loops are superimposed upon a monotonic stress vs. strain curve generated for the foam being examined. For cyclic strains of $\pm 2\%$, elliptical hysteresis loops were generated for the most part from both the untransformed and transformed foams. At $\pm 2\%$ cyclic strain, at each level of pre-strain, linear behavior of both the untransformed and transformed foams was best exhibited, as elliptical hysteresis loops. At $\pm 15\%$ cyclic strain, non-linear behavior, in the form of "boomerang" shaped hysteresis loops, were most dramatic. Between these extremes, ± 5 and $\pm 10\%$ cyclic strain, there was a gradual transition between the linear and non-linear regimes. From these results, it is observed that the orientation of the hysteresis loops is in good agreement with the slope of the stress vs. strain curves, at the level of pre-strain about which the cyclic loading was conducted.

The specific damping capacity of both the untransformed and transformed foam was determined based on the hysteresis loops generated from the various tests. The specific damping capacity is most commonly taken to be proportional to $\tan \delta$, however, this is only for materials tested in the linear regime. For cyclic loading at $\pm 15\%$ strain, both the untransformed and transformed foams exhibited non-linear behavior. The measure of specific damping capacity used was $\frac{1}{2}$, equivalent to $\tan \delta$ for the linear case according to Eq. (2).

The changes in specific damping capacity as a function of cyclic strain are given in Tables 1 and 2 and are shown in Figures 6-8. Comparison of the specific damping capacity of the

untransformed and transformed foams was based on the regions in the respective stress vs. strain curve in which the slope of this curve was similar for both types of foam. This was considered the best comparison due to the inherent differences in the stress vs. strain curve for each type of foam.

Figures 6-8 show how $\frac{E}{2}$ varies with cyclic strain for the cases of extreme tensile pre-strain, no pre-strain, and extreme compressive pre-strain. In each of these figures, only the results from the last (10th) cycle are shown. The transformed foam exhibited a higher specific damping capacity than control foam under compressive pre-strain; at large cyclic strains with no pre-strain, but not under tensile pre-strain, as shown in Fig. 6-8.

Discussion

Cellular solids⁽¹¹⁾ are composite materials in which one phase is empty space or a fluid such as water or air. Cellular solids include honeycombs, foams and other porous materials. In low density closed cell foams, the pressure of air or other gas in the pores contributes to the overall stiffness. In open cell foams, air in the pores is free to escape as the material is stressed. Under quasistatic conditions or at low frequency, flow of air has little effect. The correspondence principle of the linear theory of viscoelasticity may then be applied to the foam as a composite with one mechanically active phase. So, given⁽¹¹⁾

$$\frac{E_{\text{foam}}}{E_{\text{solid}}} = \left[\frac{\rho_{\text{foam}}}{\rho_{\text{solid}}} \right]^2, \quad (3)$$

for an elastic open cell foam (with solid referring to the solid material of which the foam is made, E as Young's modulus and ρ is density), the relationship for a corresponding viscoelastic foam is:

$$E_{\text{foam}}^* = E_{\text{solid}}^* \left[\frac{\rho_{\text{foam}}}{\rho_{\text{solid}}} \right]^2, \quad (4)$$

in which E^* is a complex quantity dependent on frequency. The loss tangent, in terms of the complex modulus is:

$$\tan \delta = \frac{\text{Im}[E^*]}{\text{Re}[E^*]}. \quad (5)$$

If one assumes, in addition to sufficiently low frequency, that no chemical changes have occurred during the foaming process then the $\tan \delta$ of a linearly viscoelastic cellular solid is that of the solid material of which it is made.

At sufficiently high frequency, significant viscoelastic loss can occur in cellular solids as a result of the viscosity of the air or water in the pores. Under quasistatic circumstances, below such frequencies, the $\tan \delta$ of the cellular solids is that of the solid material of which it is made, following the correspondence principle. At very high frequency it may be possible to set the ribs or walls of the foam into vibration, resulting in additional loss and dispersion⁽¹²⁾. The present study was conducted at too low a frequency for such effects to be important.

The discussion thus far applies to linear materials. Under large strain conditions, materials may behave nonlinearly, and new viscoelastic mechanisms including nonlinear processes in the polymer itself⁽¹³⁾ as well as friction between the ribs, may become operative.

Viscoelasticity at low frequency in foams is due to the viscoelasticity of the solid from which it is made, but in negative Poisson's ratio foams, a second causal mechanism is possible: friction between cell ribs in contact. The negative Poisson's ratio itself is not responsible for

damping; rather, the inwardly buckled structure of the re-entrant foam cells is responsible for both negative Poisson's ratio (since the cell unfolds when stretched) and for other characteristics such as altered damping. The transformed foam exhibited a higher specific damping capacity than control foam under compressive pre-strain; at large cyclic strains with no pre-strain, but not under tensile pre-strain. In tensile pre-strain, the cell ribs were not in contact to the degree they were in the more compressed mode, and therefore did not cause additional damping.

The relationship between the amount of applied pre-strain and the specific damping capacity is shown in Figures 9 and 10. For the untransformed foam the kink in the curve from 5% to 15% compressive pre-strain may be attributed to a microbuckling instability⁽¹⁴⁾ which gives rise to a banded appearance in the foam when compressed. The banding is due to the fact that in this strain regime microbuckling of the cell ribs begins and progresses, and some cell ribs come into contact giving rise to frictional damping. The transformed foam exhibits the kink near 0% compression, perhaps since the ribs are pre-buckled by the transformation process and that a frictional interaction also occurs as ribs make and break contact.

In the untransformed foam cyclically loaded at ± 5 , ± 10 , and $\pm 15\%$ strain, the specific damping capacity (based on the secant modulus energy calculation) decreased as the amplitude of cyclic loading was increased. Both transformed and untransformed foam exhibited a similar trend. At high amplitudes of cyclic loading the hysteresis loops became more asymmetric, so that the secant approach gave rise to an excessively high value of stored energy hence an underestimate of the damping. Since there is no unique way of characterizing damping in nonlinear materials, an alternate approach is described below.

As presented in the Methods section, a secant modulus was used to determine the stored energy in order to calculate $\frac{W}{V}$. A case can be made for incorporating the curvature of the plot in evaluating the stored energy, however in a nonlinear material it is not so straightforward to evaluate energy of the elastic portion. Damping was calculated for the extreme case of $\pm 15\%$ strain and the maximum tensile and compressive pre-strain, using the average of the stresses for loading and unloading to determine the stored energy. Values of damping $\frac{D}{2}$ were larger. For example in transformed foam under large compressive pre-strain $\frac{D}{2}$ was about 0.23 if calculated using the larger "triangle", and more than 0.7 if calculated using the smaller "triangle", compared with 0.13 if calculated via the secant approach. These differences associated with interpretation of stored energy are most notable for highly asymmetric loops; in the region of small pre-strain, interpretation is much more straightforward. Formal development of methods for evaluation of dimensionless damping in nonlinear materials is a topic for future effort.

The nonlinear properties of foam are relevant in a variety of applications. For example in seat cushions, pre-compression occurs as a result of the weight of the person. Moreover, the damping governs the transmission of vibration to the person, and this perception of vibration is important in automobile seats⁽¹⁴⁾. The magnitude of the damping at small amplitude, as well as the peak in damping near 10% pre-compression are comparable to results obtained in a different flexible polyurethane foam⁽¹⁵⁾.

Conclusions

The hysteresis behavior of both control (untransformed) and negative Poisson's ratio (transformed) foam were characterized at various levels of pre-strain as well as cyclic strain about a given pre-strain level. At higher levels of cyclic strain, the hysteresis loops became markedly non-linear ("boomerang shaped") for both foams. From the hysteresis loops, the specific damping capacity of the foams for each level was determined based on the ratio of energy dissipated to energy stored. Except in the case of extreme tensile pre-strain, the foams having a negative Poisson's ratio exhibited a higher value of specific damping capacity.

TABLES

Table 1. Specific Damping Capacity as a Function of Pre-Strain and Cyclic Strain for Untransformed Foams

Level of Pre-Strain	$\eta/2$ for Various Levels of Cyclic Strain			
	$\pm 2\%$	$\pm 5\%$	$\pm 10\%$	$\pm 15\%$
-65%	0.185	0.151	0.119	0.089
-50%	0.210	0.172	0.153	0.122
-15%	0.201	0.259	0.235	0.199
0%	0.161	0.174	0.157	0.131
15%	0.157	0.175	0.153	0.136
25%	0.172	0.181	0.174	0.156

Note: "-" indicates compression

Table 2. Specific Damping Capacity as a Function of Pre-Strain and Cyclic Strain for Transformed Foams

Level of Pre-Strain	$\eta/2$ for Various Levels of Cyclic Strain			
	$\pm 2\%$	$\pm 5\%$	$\pm 10\%$	$\pm 15\%$
-50%	0.212	0.189	0.158	0.131
-30%	0.198	0.197	0.164	0.145
-10%	0.161	0.157	0.132	0.117
0%	0.168	0.175	0.178	0.197
40%	0.142	0.138	0.146	0.130
60%	0.177	0.146	0.139	0.140

Note: "-" indicates compression

References

1. Lakes R. S., "Foam structures with a negative Poisson's ratio", *Science*, 235, 1987, 1038-1040
2. Friis E. A., Lakes R. S. and Park J. B., "Negative Poisson's ratio polymeric and metallic foams", *J. Materials Science*, 23, 1988, 4406-4414
3. Caddock B. D. and Evans K. E., "Microporous materials with negative Poisson's ratios: I. microstructure and mechanical properties", *Journal of Physics D: Applied Physics*, 22, 1989, 1877-1882
4. Evans K. E. and Caddock B. D., "Microporous materials with negative Poisson's ratios: II. mechanisms and interpretation", *Journal of Physics D: Applied Physics*, 22, 1989, 1883-1887
5. Alderson K. L. and Evans K. E., "The fabrication of microporous polyethylene having a negative Poisson's ratio", *Polymer*, 33, 1992, 4435-4438
6. Graesser E. J. and Wong C. R., The relationship of traditional damping measures for materials with high damping capacity: a review. In *M³D: Mechanics and Mechanisms of Material Damping*, (edited by Kinra V. K. and Wolfenden A.), ASTM, Philadelphia, 1992
7. Ferry J. D., *Viscoelastic Properties of Polymers*, 2nd ed., J. Wiley, NY, 1970
8. Nashif A. D., Jones D. I. G. and Henderson J. P., *Vibration Damping*, J. Wiley, NY, 1985
9. Lazan B. L., *Damping of Materials and Members in Structural Mechanics*, Pergamon, NY, 1968
10. Choi J. B. and Lakes R. S., "Non-linear properties of polymer cellular materials with a negative Poisson's ratio", *Journal of Materials Science*, 27, 1992, 4678-4684
11. Gibson L. J. and Ashby M. F., *Cellular Solids*, Pergamon, 1988
12. Chen C. P. and Lakes R. S., "Dynamic wave dispersion and loss properties of conventional and negative Poisson's ratio polymeric cellular materials", *Cellular Polymers*, 8, 1989, 343-359
13. Hilyard N. C., Hysteresis and energy loss in flexible polyurethane foams. In *Low Density Plastics*, (edited by Hilyard N. C. and Cunningham A.), Chapman and Hall, London, 1994.
14. Rosakis, P., Ruina, A., and Lakes, R.S., "Microbuckling instability in elastomeric cellular solids", *J. Materials Science*, 28, 1993, 4667-4672.
15. Cunningham A., Huygens E. and Leenslag J. W., "MDI comfort cushioning for automotive applications", *Cellular Polymers*, 13, 1994, 461-472
16. Lakes R. S., *Viscoelastic Solids*, CRC Press, Boca Raton, FL, 1998.

FIGURES

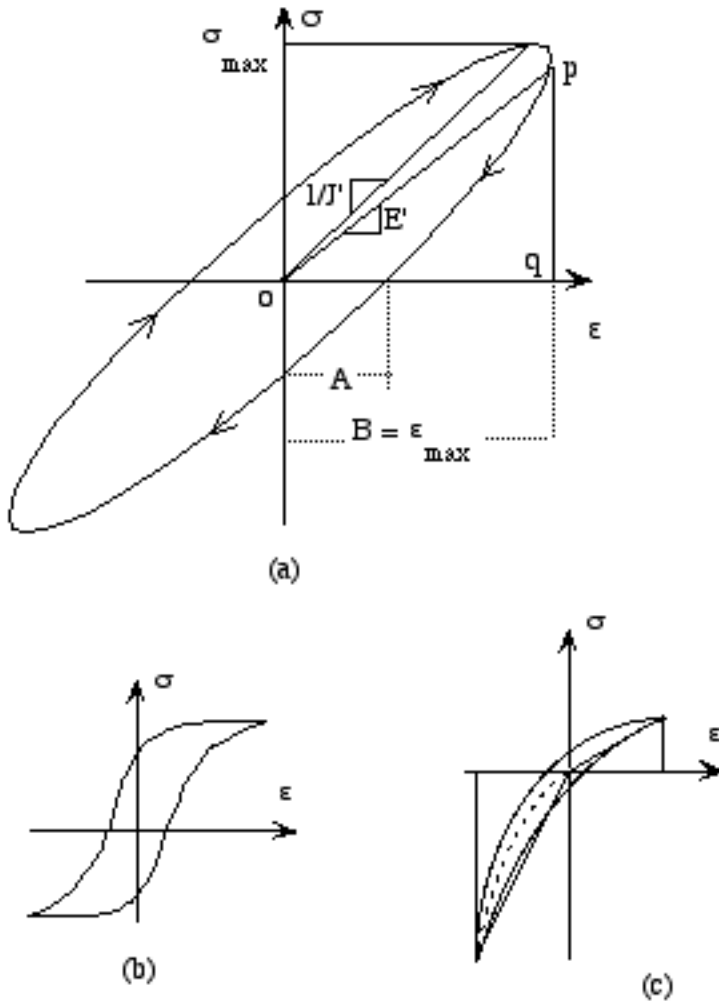


Figure 1. Stress vs. strain for viscoelastic materials under cyclic loading.

- (a) Linear material exhibits an elliptic loop⁽¹⁶⁾.
- (b) A nonlinear material.
- (c) Another nonlinear material.

Figure 2. Hysteresis loops for the untransformed foam at various levels of pre-strain, with cyclic loading at $\pm 2\%$. The hysteresis loops (magnification = 5x) from the 10th cycle are shown.

Figure 3. Hysteresis loops for the untransformed foam at various levels of pre-strain, with cyclic loading at $\pm 15\%$. The hysteresis loops (magnification = 1x) from the 10th cycle are shown.

Figure 4. Hysteresis loops for the negative Poisson's ratio foam at various levels of pre-strain, with cyclic loading at $\pm 2\%$. The hysteresis loops (magnification = 5x) from the 10th cycle are shown.

Figure 5. Hysteresis loops for the negative Poisson's ratio foam at various levels of pre-strain, with cyclic loading at $\pm 15\%$. The hysteresis loops (magnification = 1x) from the 10th cycle are shown.

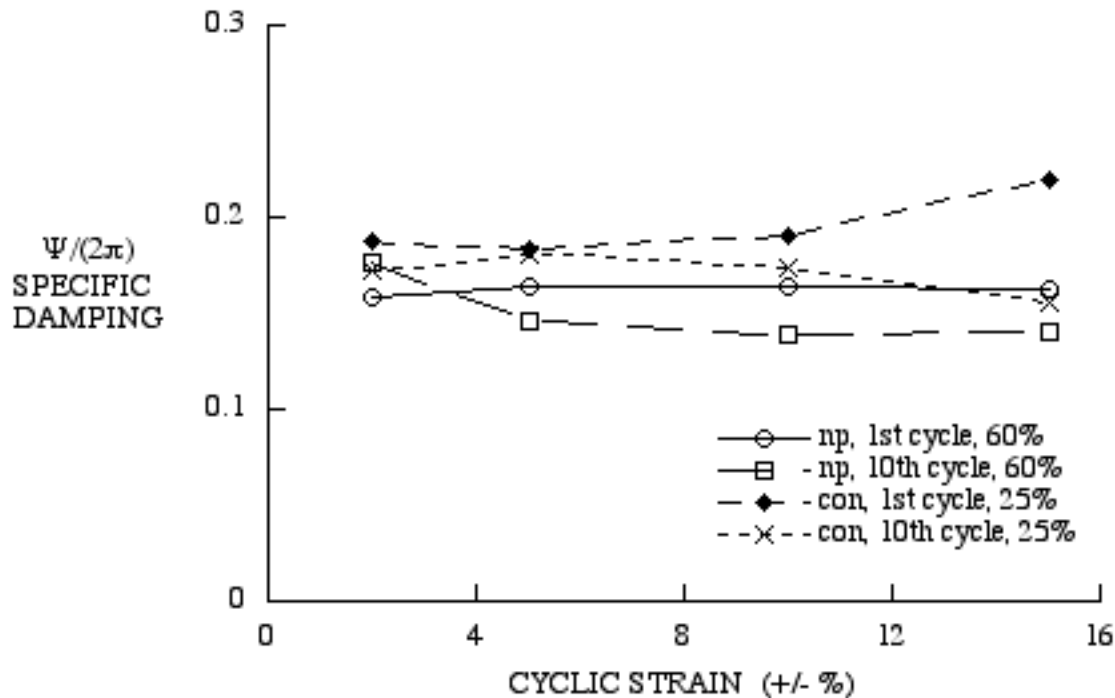


Figure 6. A comparison of the negative Poisson's ratio foam and the control foam at a specified tensile pre-strain is shown. The specific damping capacity, $\Psi/(2\pi)$, as a function of cyclic strain is presented. The transformed foam with a resultant negative Poisson's ratio is designated by "np" and the untransformed foam is designated by "con".

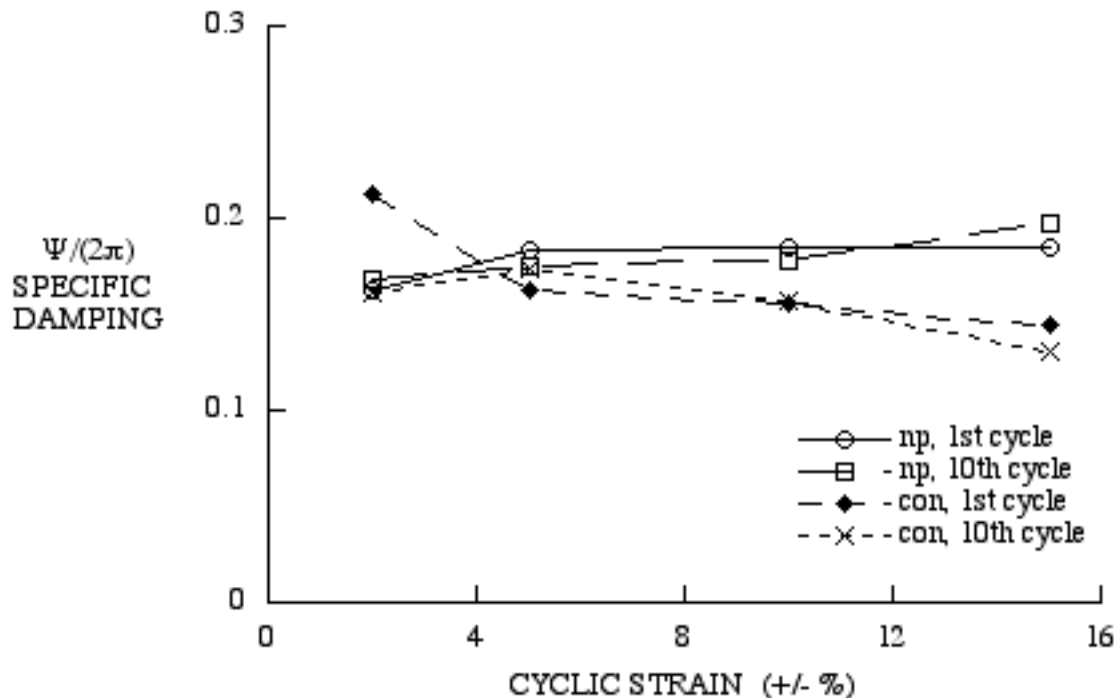


Figure 7. A comparison of the negative Poisson's ratio foam and the control foam with no pre-strain is shown. The specific damping capacity, $\Psi/(2\pi)$, as a function of cyclic strain is presented. The transformed foam with a resultant negative Poisson's ratio is designated by "np" and the untransformed foam is designated by "con".

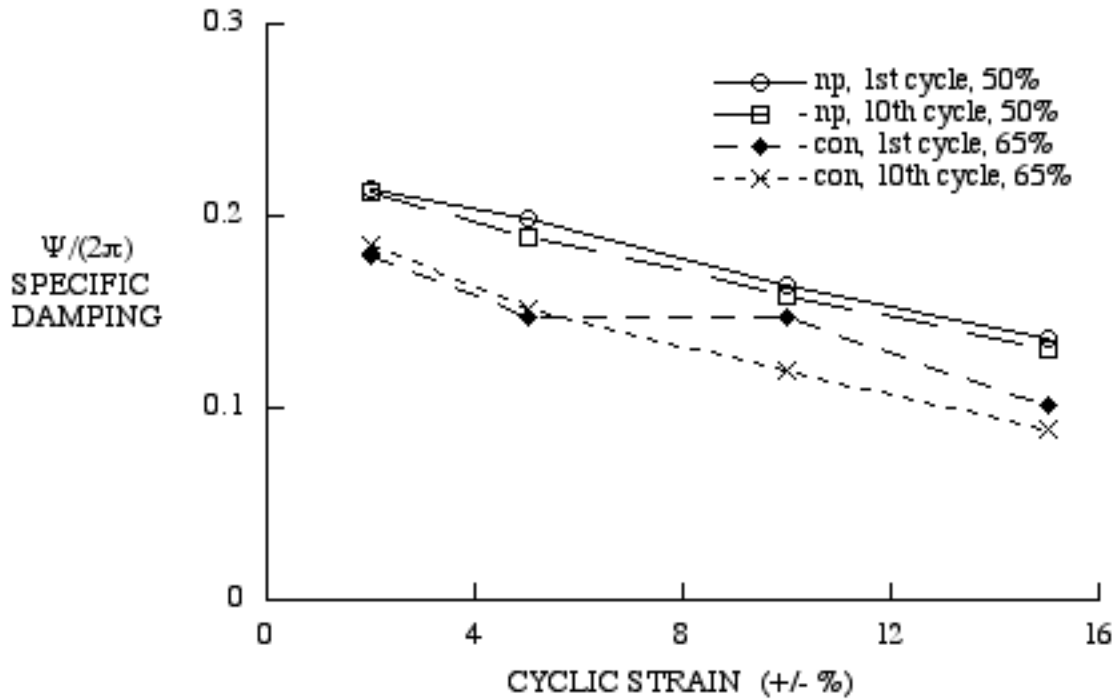


Figure 8. A comparison of the negative Poisson's ratio foam and the control foam at a specified compressive pre-strain is shown. The specific damping capacity, $\Psi/(2\pi)$, as a function of cyclic strain is presented. The transformed foam with a resultant negative Poisson's ratio is designated by "np" and the untransformed foam is designated by "con".

Figure 9. Specific damping as a function of applied pre-strain and cyclic strain for the untransformed foam.

Figure 10. Specific damping as a function of applied pre-strain and cyclic strain for the transformed foam.